Bioelectrochemistry 78 (2010) 106–112

Contents lists available at ScienceDirect

Bioelectrochemistry

journal homepage: www.elsevier.com/locate/bioelechem

Direct electron transfer and electrocatalysis of hemoglobin in ZnO coated multiwalled carbon nanotubes and Nafion composite matrix

Wei Ma, Danbi Tian *

College of Science, Nanjing University of Technology, Nanjing 210009, PR China

ARTICLE INFO

Article history:
Received 9 October 2008
Received in revised form 5 August 2009
Accepted 9 August 2009
Available online 17 August 2009

Keywords:
Hemoglobin
ZnO
Multiwalled carbon nanotubes
Nafion
Bioelectrochemistry

ABSTRACT

ZnO coated multiwalled carbon nanotubes (ZnO-MWCNTs) nano-composite was synthesized by the hydrothermal method and expected to offer a promising template for biosensor fabrication due to satisfying biocompatibility and improved properties. The ZnO-MWCNTs nano-composite was mixed with Nafion solution to form a composite matrix for the fabrication of hemoglobin (Hb) biosensor. This composite matrix combined the advantages of inorganic composite (ZnO-MWCNTs) and organic polymer (Nafion) and could promote the direct electron transfer of Hb. The Hb/ZnO-MWCNTs/Nafion film exhibited a pair of well-defined, quasi-reversible redox peaks with a formal potential of −0.353 V (vs. SCE), characteristic of heme redox couple (Fe(III)/Fe(II)) of Hb. Hb retained its near-native conformation in the composite film. The immobilized Hb showed fast and excellent electrocatalytic activity to H_2O_2 with a linear range from 2×10^{-7} to 1.2×10^{-5} M, and the detection limit was 8.4×10^{-8} M. The sensitivity and apparent Michaelis–Menten constant were 1.31 A/(M·cm^2) and 82.8 μM, respectively, which indicated that Hb had a high affinity to H_2O_2. This biosensor also showed excellent electrocatalytic activity towards trichloroacetic acid.

1. Introduction

Direct electron transfer of redox proteins not only provide a model for the study of electron transport of proteins in biological system which is important to understand the material metabolism and energy transformation in the life process, but also establish a foundation for fabricating third generation of electrochemical biosensors [1]. Hemoglobin (Hb) is considered as an ideal model molecule to study the direct electron transfer of protein due to its commercial availability and relatively well know structure [2]. However, Hb usually cannot exhibit heterogeneous electron-transfer processes in most cases owing to its large protein size and the inaccessibility of the electroactive center which is deeply buried in the electrochemical insulted peptide backbone [3]. Up to now, great efforts have been taken to obtain the direct electron transfer of Hb [4–9].

Nanotechnology has provided a novel way to enhance electron-transfer rate between Hb and electrode due to the quantum size effect and surface effect. Many nanomaterials have been used to immobilize Hb on the surface of electrode, such as nano gold [10], carbon nanotubes (CNTs) [11], quantum dots [12], and porous nanomaterials [13]. CNTs have been used to fabricate sensors and biosensors due to their unique electronic, structural, mechanical, and electromechanical properties and biocompatibility [14,15]. Many proteins immobilizing on the CNTs have realized direct electron transfer [11]. ZnO is a very important wide-band-gap semiconductor with a room-temperature wide band gap of 3.37 eV [16]. Owing to its biomimetic and high electro communication features, nano ZnO has great prospective application in the biosensors [17,18]. Recently, ZnO nanorods have been used to fabricate reagentless uric acid biosensor [19], and electrodeposited nanoporous ZnO film has been used to immobilize Mb to realize direct electron transfer, suggesting that ZnO is a promising matrix to develop biosensors [20]. The nano-composite [21] of multiwalled carbon nanotubes (MWCNTs) coated with ZnO may have an interesting application in biosensor due to the synergic effect of ZnO and MWCNTs.

Nafion has good electrical conductivity, good biocompatibility, excellent film forming and adhesion ability, high chemical stability and ability to resist interferences from anions and biological macromolecules, which make it a good matrix for biomolecule immobilization [22,23].

In this work, we constructed a novel Hb biosensor based on the ZnO-MWCNTs/Nafion inorganic–organic composite film as the immobilization matrix. This composite matrix combined the advantages of inorganic composite (ZnO-MWCNTs) and organic polymer (Nafion), which could promote the direct electron transfer of Hb. ZnO-MWCNTs nano-composite was synthesized by the hydrothermal method, and we expected that the combination of ZnO and MWCNTs may induce interesting charge transfer and enhance the electrocatalytic activity of enzymatic bioelectrode. The direct electron transfer between Hb and glassy carbon electrode (GCE) was realized

* Corresponding author. Tel.: +86 25 8358 7428; fax: +86 25 8358 7443.
E-mail address: danbi@njut.edu.cn (D. Tian).

1567-5394/$ – see front matter.
doi:10.1016/j.bioelechem.2009.08.002

in this biosensor. The results showed that the immobilized Hb almost retained its native structure and displayed high electroactivity and electrocatalytic response to H_2O_2 and trichloroacetic acid (TCA). The biosensor had high stability and satisfactory reproducibility. This demonstrates that the composite matrix is suitable for the immobilization of Hb and has potential application in the construction of biosensors.

2. Experimental

2.1. Chemicals and apparatus

MWCNTs with diameters of about 30 nm were provided by Shenzhen Nanotech Port Co. Ltd. Hb (bovine blood) was obtained from Sigma and was used as received without further purification. Nafion (5% in a mixture of lower aliphatic alcohols and water) was purchased from Sigma. Trichloroacetic acid (TCA) and H_2O_2 (30% w/w solution) were purchased from Shanghai Chemical Reagent Company. The supporting electrolyte was 0.1 M phosphate buffer solution (PBS), which was prepared with Na_2HPO_4 and NaH_2PO_4. Various pH were adjusted with 0.1 M NaOH or 0.1 M H_3PO_4 solution. All other chemicals were of analytical grade and used without further purification. All solutions were prepared with twice-distilled water.

2.2. Preparation of ZnO-MWCNTs nano-composite

MWCNTs were oxidized in concentrated HNO_3 by refluxing for 8 h at 140 °C. This cut the MWCNTs into shorter tubes and also opened up carboxylic groups and hydroxyl groups on the sidewalls [24].

5 mg of acid-treated MWCNTs were added to 20 mL of the mixture of anhydrous ethanol and twice-distilled water (1:1, V/V) under ultrasonic irradiation for 30 min to ensure good dispersion, then 5 mL of 0.02 M zinc acetate solution was added to the mixture under constant stirring. Then concentrated ammonia was added until the pH of the mixture solution was about 9–10. After continuously agitation for another 2 h, the mixture was filtered and the solid was redispersed in 20 mL of twice-distilled water, then the mixture was transferred to a Teflon-lined stainless steel autoclave and placed inside an electric oven at 150 °C for 5 h. After the synthesis, the solid product recovered by filter was washed several times with twice-distilled water and dried in vacuum.

2.3. Construction of the biosensor

A GCE (3 mm diameter) was polished with 1.0, 0.3 and 0.05 μm alumina powder, respectively, rinsed thoroughly with twice-distilled water between each polishing step, and followed by sonication in acetone and twice-distilled water successively. After these pretreatments, the electrode was allowed to dry at room temperature. For preparation of Hb electrodes, solution of Hb (5 mg/mL) was prepared in 0.1 M PBS (pH 8.0). 500 μL of ZnO-MWCNTs (1 mg/mL) suspension was mixed with 300 μL of Hb solution and 200 μL of 1 wt% Nafion solution. The mixture was hand-mixed thoroughly. The resulting suspension (5.0 μL) was deposited onto the electrode surface. The casted GCE was left to dry in a sealed case and stored at 4 °C when not in use.

2.4. Instruments

UV–VIS absorption spectra were recorded with Agilent 8453 UV–visible spectroscopy system. FT-IR spectra were obtained on an AVATAR370 (Nicolet) FT-IR instrument. Raman spectrum was performed using Renishaw inVia Raman spectrometer. Transmission electron microscope (TEM) measurements were recorded on a JEOL JEM-1010 transmission electron microscope, using an accelerating voltage of 100 kV.

Electrochemical measurements were performed on a CHI660C electrochemical workstation (Shanghai Chenhua, Shanghai, China). All electrochemical experiments were carried out in a conventional three-electrode system using a modified GCE as working electrode, a platinum wire as counter electrode, and a saturated calomel electrode (SCE, standard electrode potential is 0.2412 V at the temperature of 298.15K) as reference electrode. The PBS was purged with high-purity nitrogen for 30 min prior to experiments and a nitrogen environment was then kept over the solution in the cell.

3. Results and discussion

3.1. TEM and Raman spectrum measurements of ZnO-MWCNTs nano-composite

Fig. 1 shows the TEM images of MWCNTs before (Fig. 1A) and after (Fig. 1B) coating with ZnO thin film. When MWCNTs were coated with ZnO, the diameters of MWCNTs were larger than those of pristine acid-treated MWCNTs. The interface between MWCNTs and ZnO could clearly be observed, indicating that ZnO were well attached on the outermost shell of MWCNTs.

Fig. 2A shows the Raman spectrum of MWCNTs (Fig. 2A, curve a) and ZnO-MWCNTs (Fig. 2A, curve b). There were no obvious absorption peaks in the Raman spectrum of MWCNTs between 250 and 550 cm^{-1}. It clearly showed that there were two absorption peaks at around 328 and 435 cm^{-1} in the Raman spectrum of ZnO-MWCNTs, which originated from the oscillation of Zn–O in ZnO [25]. The

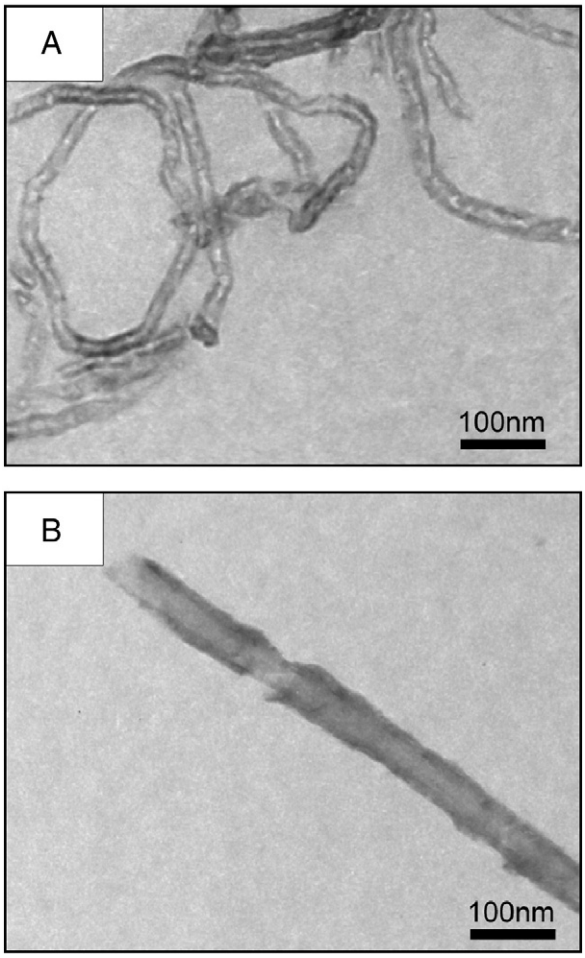

Fig. 1. TEM images of acid-MWCNTs (A) and ZnO-MWCNTs nano-composites (B).

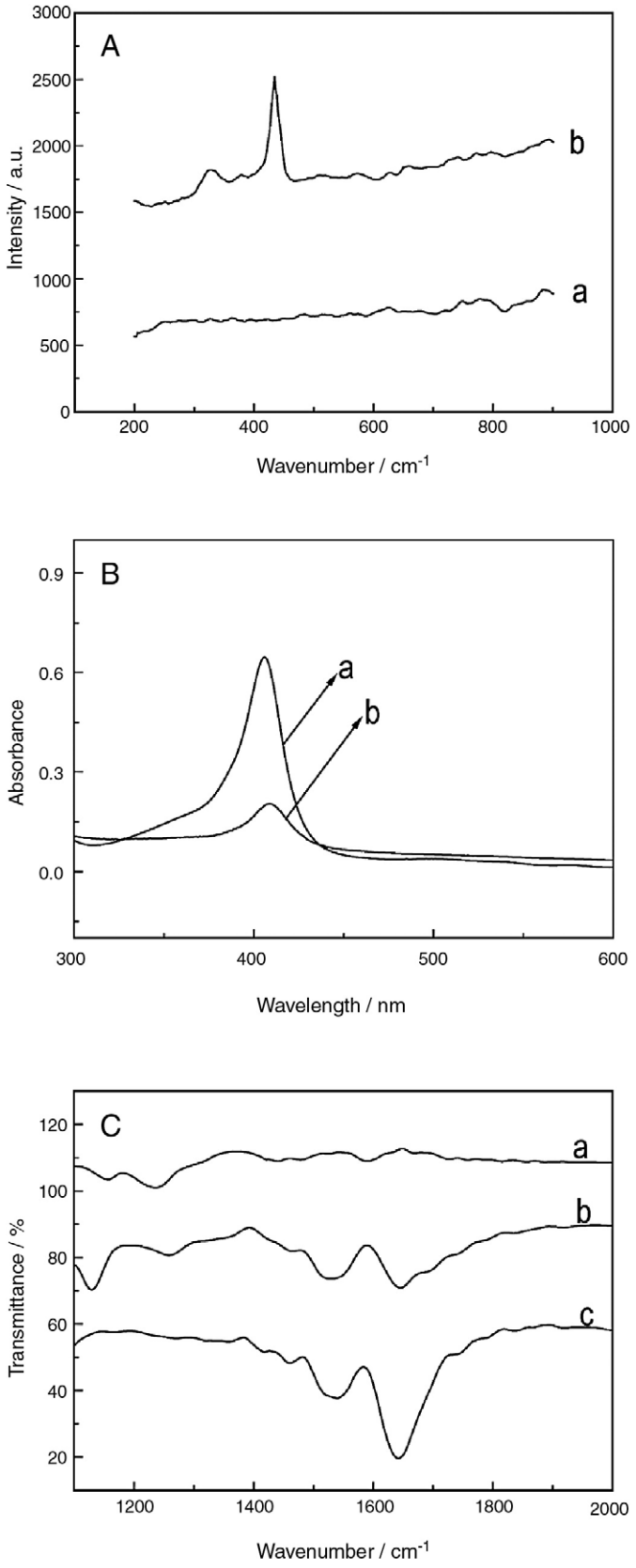

Fig. 2. A. Raman spectrum of MWCNTs (a) and ZnO-MWCNTs (b); B. UV–VIS spectra of Hb in 7.0 PBS (a) and Hb in ZnO-MWCNTs/Nafion suspension (b); C. FT-IR spectra of ZnO-MWCNTs/Nafion (a), Hb/ZnO-MWCNTs/Nafion (b) and Hb (c).

broadening asymmetry Raman peak at 435 cm^{-1} was typical of ZnO Raman active branches, which was attributed to the E2 mode of ZnO [26].

3.2. UV–VIS spectroscopic analysis

The Soret band of heme protein is usually an indicator of the microenvironment where heme center locates and can give helpful information on whether proteins have been denatured [27]. UV–VIS spectroscopy is a useful tool for monitoring the possible change of the Soret adsorption band in the heme group region. As shown in Fig. 2B, the Soret absorption of Hb in ZnO-MWCNTs/Nafion suspension was located at 409 nm, which was close to that of native Hb (i.e. 406 nm), suggesting that no significant denaturation of the immobilized Hb occurred.

3.3. FT-IR characterization of Hb/ZnO-MWCNTs/Nafion composite film

FT-IR spectroscopy is an effective means to explore the secondary structure of proteins [28]. The characteristic amide I and II bands of proteins provide detailed information of the secondary structure of polypeptide chain. The amide I band (1700–1600 cm^{-1}) is attributed to the C O stretching vibrations of peptide linkages in the backbone of the protein. The amide II band (1600–1500 cm^{-1}) is attributed to the combination of N–H bending and C–N stretching of the peptide groups [29]. Fig. 2C shows the FT-IR spectra of the Hb, the Hb/ZnO-MWCNTs/Nafion and the ZnO-MWCNTs/Nafion composite film. As shown in Fig. 2C, curves b and c, the amide I and II bands of Hb in the ZnO-MWCNTs/Nafion composite film were located at 1645.1 and 1537.1 cm^{-1}, which had similar shapes to that of the native Hb, except a slight shift to the native Hb (1641.8 and 1540.2 cm^{-1}). This indicated that Hb was absorbed onto the ZnO-MWCNTs/Nafion composite film and suggested the existence of an interaction between Hb and ZnO-MWCNTs/Nafion. The denatured protein does not show such peaks [30]. It should be noted that the ZnO-MWCNTs/Nafion composite film showed an FT-IR absorption band (1589.1 cm^{-1}) between amide band I and amide II region of Hb, as shown in Fig. 2C, curve a, which was the characteristic peak of carboxylic ion. However, the absorption band (1589.1 cm^{-1}) was not consistent with that of the Hb. The above results suggested that the Hb retained its native secondary structure in the ZnO-MWCNTs/Nafion composite film. The ZnO-MWCNTs/Nafion composite film may provide a promising matrix for enzyme immobilization because of its satisfying biocompatibility.

3.4. Direct electron transfer of Hb/ZnO-MWCNTs/Nafion/GCE

Fig. 3 shows the typical cyclic voltammograms (CVs) of the Hb/ZnO-MWCNTs/Nafion/GCE (a), Hb/Nafion/GCE (b), Hb/GCE (c), ZnO-MWCNTs/Nafion/GCE (d) and Hb/MWCNTs/Nafion/GCE (e). A wide peak (Fig. 3d) was observed in pH 7.0 PBS, which was attributed to the redox of carboxylic groups in some carboxylic MWCNTs which were not coated with ZnO completely [31]. When the electrode was modified with Hb, only an irreversible and small reduction peak was observed (Fig. 3c). A pair of stable and well-defined redox peaks of Hb for the Hb (Fe^{III})/Hb(Fe^{II}) redox couple transformation, which could be ascribed to the electron transfer between the Hb and the underlying electrode, was observed at the Hb/ZnO-MWCNTs/Nafion/GCE (Fig. 3a). The anodic and cathodic peak potentials were located at −0.317 and −0.388 V (vs. SCE), respectively. And the potential difference between the two peaks, ΔE_p, was 71 mV at a scan rate of 100 mV/s, which indicated that Hb undergone a quasi-reversible redox progress at the modified electrode. The formal potential ($E^{0'}$) calculated by averaging the anodic and cathodic peak potentials was −0.353 V (vs. SCE), which agreed well with other Hb modified electrodes [4,32]. Compared with Hb/ZnO-MWCNTs/Nafion/GCE, the redox peaks observed at the Hb/Nafion/GCE (Fig. 3b) were much smaller, while the Hb/MWCNTs/Nafion/GCE

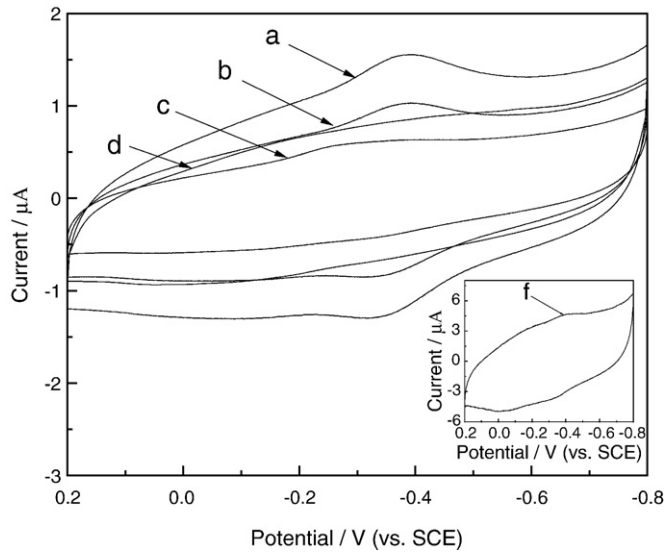

Fig. 3. Cyclic voltammograms of Hb/ZnO-MWCNTs/Nafion/GCE (a), Hb/Nafion/GCE (b), Hb/GCE (c), ZnO-MWCNTs/Nafion/GCE (d) and Hb/MWCNTs/Nafion/GCE (e) in 0.1 M PBS (pH 7.0) at a scan rate of 100 mV/s.

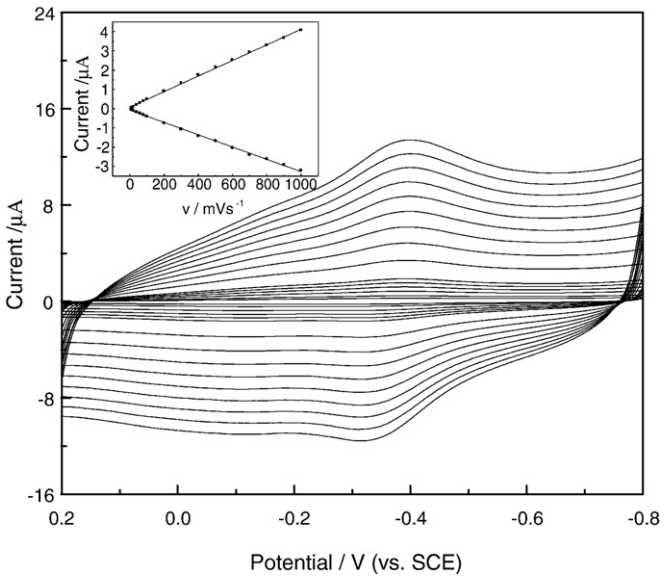

Fig. 4. Cyclic voltammograms of Hb/ZnO-MWCNTs/Nafion/GCE in 0.1 M PBS (pH 7.0) with scan rates of 10–1000 mV/s. Inset: plot of peak current vs. scan rate.

exhibited a pair of undefined redox peaks of Hb (Fig. 3e). It revealed that ZnO-MWCNTs played an important role in facilitating the direct electron transfer of Hb by the synergism with Nafion.

Fig. 4 shows the CVs of the modified electrode at different scan rates. With the increase of the scan rate, the redox peak current and the peak separation (ΔE_p) increased simultaneously. Both anodic and cathodic peak currents increased linearly with scan rates from 10 to 1000 mV/s (inset in Fig. 4), and it was clear that Hb adsorbed onto the surface undergone a surface-confined electron transfer. The plot of lg (I_p/μA) vs. lg (v/mV/s) gave a straight line with a slope of 0.94, which was characteristic of a thin-layer electrochemical process [20]. For such a surface process, the average surface coverage (Γ^*) can be calculated according to the Laviron equation [33],

$$I_p = \frac{n^2F^2v\Gamma^*A}{4RT} = \frac{nFQv}{4RT} \quad (1)$$

where v is the sweep rate, A is the effective surface area (7.1×10^{-6} m^2) of the modified electrode, I_p is the peak current, Q is the quantity of charge, n is number of electron transferred in the electrode reaction, R is mol gas constant, F is Faraday constant, and T is the temperature (298.15K). The number of electrons transferred for the direct electron transfer reaction of Hb was calculated to be $n=0.95$, suggesting that a single electron-transfer reaction occurred at the Hb/ZnO-MWCNTs/Nafion/GCE. From the slope of the I_p–v curve, Γ^* of Hb on ZnO-MWCNTs/Nafion/GCE was estimated to be 5.82×10^{-11} mol/cm^2, which was larger than the theoretical monolayer coverage of Hb (ca. 1.89×10^{-11} mol/cm^2). This value showed that a multilayer of proteins participated in the electron-transfer process in the three-dimension composite.

According to the Laviron theory, the transfer coefficient (α) and electron-transfer rate constant (k_s) can be estimated by measuring the variation of peak potential with scan rate [34]. The transfer coefficient (α) and electron-transfer rate constant (k_s) were 0.46 and 1.14 s^{-1}, respectively. The value for electron-transfer rate constant was higher than electron-transfer rate constant of Hb in silica-coated gold nanorods, 0.83 s^{-1} [35], carbon nanotubes, 0.062 s^{-1} [36], and Au-SBA-15, 0.8 s^{-1} [37]. This value showed that the electron transfer of Hb in ZnO-MWCNTs/Nafion composite film was facile. It is assumed that the nanomaterials increase the surface area and active point for adsorbing Hb. Nano ZnO has good biocompatibility and Zn has coordinative affinity for the oxygen of the carboxylic group of the amino acids in Hb [38], which could retain the bioactivity of Hb. The ZnO-MWCNTs/Nafion composite film electrode possessed a three-dimensional architecture, in which each separated one dimensional ZnO-MWCNTs nano-composite behaved like an individual nanoelectrode, which enhanced the direct electron transfer of Hb.

CVs of Hb/ZnO-MWCNTs/Nafion/GCE showed a strong dependence on pH of external solution. As shown in Fig. 5, both the anodic and cathodic peak potentials shifted negatively with increasing pH from 4.0 to 9.0. The same voltammogram can be obtained when the modified GCE was transferred from a solution with different pH back to the pH 7.0 PBS. Here, the formal potential ($E^{0'}$) showed linearly a response to pH from 4.0 to 9.0. The linear regression equation was $y(\mathrm{V}) = -0.0434x\ (\mathrm{V/pH}) - 0.0718\ (R^2 = 0.992)$. The slope was about −43.4 mV/pH, which was a little smaller than the theoretical value of −58 mV/pH at 18 °C for a reversible proton-coupled single electron-transfer process [39], and this may be that the protonation of trans-ligands influences the heme iron and amino acids around the Hb

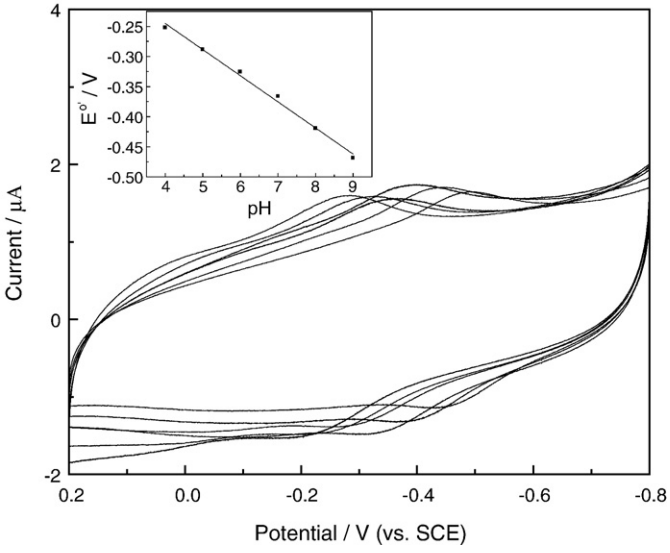

Fig. 5. Cyclic voltammograms of Hb/ZnO-MWCNTs/Nafion/GCE in 0.1 M PBS at different pH, from left to right 4.0 to 9.0 at a scan rate of 100 mV/s. Inset: plot of formal potential vs. pH.

or that the protonation of the water molecules coordinated to the central iron [40]. Thus, the electrochemical reduction reaction of Hb may be described as follows [41]:

$$Hb(Fe^{III}) + H^+ + e^- \rightarrow Hb(Fe^{II}). \quad (2)$$

3.5. Electrocatalytic properties of Hb/ZnO-MWCNTs/Nafion/GCE

As is well known, Hb is a kind of heme (Fe) protein, which has a good electrocatalytic activity to many reductive materials. Here, TCA and H_2O_2 served as models to investigate the electrocatalytic properties of the Hb/ZnO-MWCNTs/Nafion/GCE.

3.5.1. Electrocatalytic reduction of TCA.

TCA is an important organohalide environmental pollutant and to detect the concentration of TCA in the environment is of great importance for controlling pollution. Fig. 6 shows CVs of the electrocatalytic reduction of TCA by this biosensor. When TCA was added to a pH 5.5 PBS, an increase in the reduction peak was observed at about −0.320 V (vs. SCE) (Fig. 6d), accompanying the decrease of the oxidation peak. However, at the same potential window, this phenomenon could not be observed on ZnO-MWCNTs/Nafion film (Fig. 6b). These results were consistent with the reduction of TCA by $Hb(Fe^{II})$ in a catalytic cycle, presumably resulting in the reductive dechlorination of TCA [42]. The mechanism of this electrocatalytic reduction process can be rationalized as follows [4]:

$$Hb(Fe^{III}) + e^- \rightarrow Hb(Fe^{II}) \quad (3)$$

$$Hb(Fe^{II}) + CCl_3COOH + H^+ + e^- \rightarrow Hb(Fe^{III}) + HCCl_2COOH + Cl^-. \quad (4)$$

The reduction peak current increased with increasing TCA concentration (Figs. 6d–f). The linear response range of the biosensor to the TCA concentration was from 1 mM to 82.6 mM as seen in the inset of Fig. 8. The linear regression equation was $I(\mu A) = 0.0818C\ (mM) + 0.103$ ($R^2 = 0.999$). The detection limit (S/N = 3) of this biosensor towards TCA was 0.8 mM, which was lower than 1.98 mM [43], and 10 mM [44]. All these data indicated that this biosensor could be used to detect organohalide pollutants in the environment.

3.5.2. Electrocatalytic reduction of H_2O_2

The elecrocatalytic reactivity of Hb/ZnO-MWCNTs/Nafion modified electrode towards H_2O_2 was investigated by CVs. As shown in Fig. 7, when H_2O_2 was added to PBS (pH 7.0), an increase of the reduction peak at about −0.390 V (vs. SCE) was seen with the decrease of the oxidation peak (Fig. 7f). No peaks were observed at the ZnO-MWCNTs/Nafion/GCE in the presence of H_2O_2 (Fig. 7b). The reduction peak current (i_{pc}) value increases with the increasing concentration of H_2O_2 added (Figs. 7d–i), which was characteristic of the electrocatalytic reduction of H_2O_2 by Hb immobilized in the composite film. The linear response range of the biosensor to the H_2O_2 concentration was from 1×10^{-6} M to 8×10^{-5} M as seen in the inset of Fig. 7. The linear regression equation was $I(\mu A) = 0.01C\ (\mu M) + 0.02$ ($R^2 = 0.999$). The detection limit (S/N = 3) of this biosensor towards H_2O_2 was 8.5×10^{-7} M.

The electrocatalytic reduction of H_2O_2 was also studied by amperometry (Fig. 8). Upon addition of H_2O_2 to the PBS, a stepwise growth of reduction current was observed. The modified GCE achieved 95% of the steady current towards H_2O_2 in less than 3 s, which indicated that the electrocatalytic response was very fast. The amperometric current had a good linear relationship with the concentration of H_2O_2 in the range of 2×10^{-7} to 1.2×10^{-5} M and the linear regression equation was $I(\mu A) = 0.102C\ (\mu M) + 0.023$ ($R^2 = 0.9985$, $n = 26$). From the slope, the detection limit to H_2O_2 (S/N = 3) was estimated to be 8.4×10^{-8} M. The sensitivity of this biosensor was calculated to be 1.31 A/(M·cm^2), which was much higher than those of Hb at ZrO_2/DMSO, 0.74 A/(M·cm^2) [45], and Prussian Blue/Nafion, 0.6 A/(M·cm^2) [46]. When the concentration of H_2O_2 was higher than 1.2×10^{-5} M, a response platform was observed, showing a characteristic of the Michaelis–Menten kinetic mechanism. The apparent Michaelis–Menten constant (K_m^{app}), which is a reflection of the enzyme–substrate kinetics, is calculated by the Lineweaver–Burk equation [47]:

$$1/I_{ss} = 1/I_{max} + K_m^{app}/I_{max}C \quad (5)$$

where I_{ss} is the steady current after the addition of substrate, C is the bulk concentration of the substrate and I_{max} is the maximum current measured under the saturated substrate condition. The apparent Michaelis–Menten constant (K_m^{app}) in this work was 82.8 μM, implying that this biosensor exhibited a high affinity to H_2O_2. This value was smaller than those of Hb immobilized onto ZrO_2, 1.77 mM [48], Hb

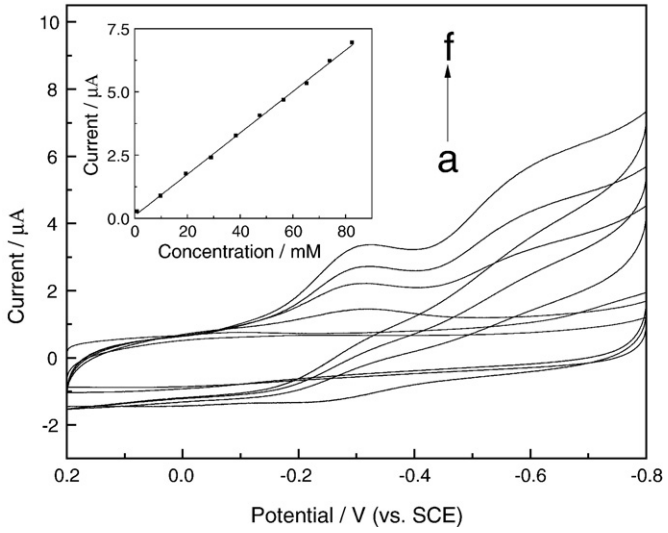

Fig. 6. Cyclic voltammograms of ZnO-MWCNTs/Nafion/GCE in a 0.1 M PBS (pH 5.5) without (a) and with 9.9 mM TCA (b). Cyclic voltammograms of Hb/ZnO-MWCNTs/Nafion/GCE in a 0.1 M PBS (pH 5.5) without (c) and with 9.9, 19.6 and 29.1 mM TCA (d–f). Scan rate: 100 mV/s. Inset: the catalytic response vs. TCA concentration.

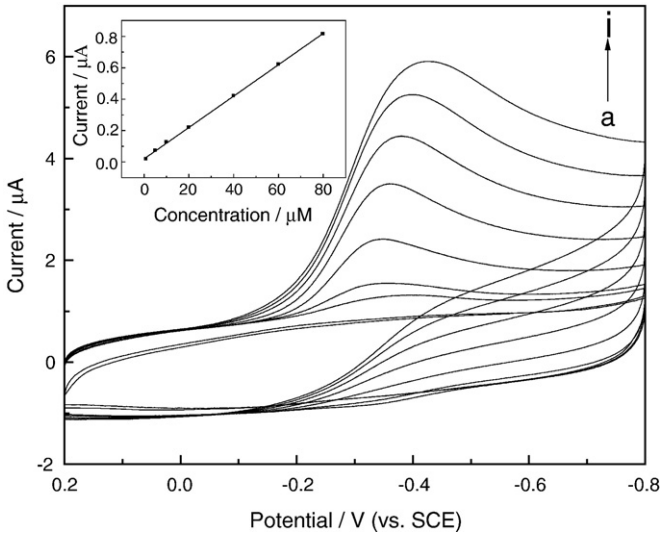

Fig. 7. Cyclic voltammograms of ZnO-MWCNTs/Nafion/GCE in a 0.1 M PBS (pH 7.0) without (a) and with 0.08 mM H_2O_2 (b). Cyclic voltammograms of Hb/ZnO-MWCNTs/Nafion/GCE in a 0.1 M PBS (pH 7.0) without (c) and with 0.01, 0.04, 0.08, 0.12, 0.16 and 0.2 mM H_2O_2 (d–i). Scan rate: 100 mV/s. Inset: the catalytic response vs. H_2O_2 concentration.

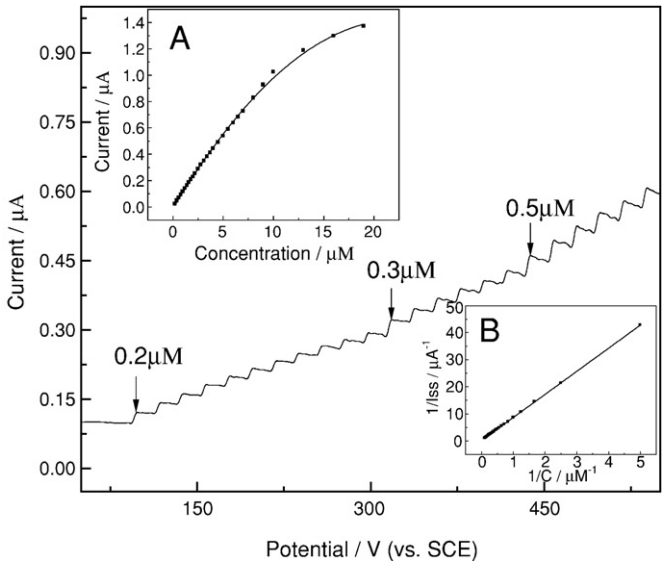

Fig. 8. Amperometric response of Hb/ZnO-MWCNTs/Nafion/GCE at −0.39 V upon successive addition of H_2O_2 into 0.1 M PBS (pH 7.0) while stirring. Inset: plot of chronoamperometric current vs. H_2O_2 concentration (A), recorded plot for determination of K_m^{app} (B).

immobilized in cobalt oxide particles, 0.385 mM [49], Hb entrapped in chitosan and $CaCO_3$ nanoparticles, 0.75 mM [50], and Hb in a SP Sophadex membrane, 1.9 mM [6]. It clearly showed that the activity of Hb in the ZnO-MWCNTs/Nafion film was greatly enhanced and Hb had a large catalytic activity towards H_2O_2.This could be ascribed to that the Hb molecules could tightly absorbed onto ZnO-MWCNTs with relative favoranle orientation by the electrostatic force, which was beneficial for the realization of the whole activity of Hb. Choi et al. [51] proposed that an addition of a moderately hydrophobic Nafion polymer into the silica sol-gel was advantageous to maintain optimum enzyme activity such as tyrosinase in the composite film. Since Nafion was biocompatible, the presence of Nafion in the biocomposite film not only made the film uniform but also led to the increased activity of Hb. The smaller K_m^{app} value indicates that the diffusion of substrate and product into and out of the membrane is slightly easier. The faster diffusion of substrates and products into and out of the membrane is possible through the interconnected porous channels in the composite films [51]. The ZnO-MWCNTs/Nafion composite film electrode possessed a three-dimensional network architecture, which could make the substrates and products have faster diffusion and improve the catalytic activity.

For comparison, other reported protein films were listed in Table 1. The Hb/ZnO-MWCNTs/Nafion film presented excellent analytical performance in the determination of H_2O_2.

Table 1
Peroxidase-like activity of some Hb films.

Film	Linear range (μM)	Detection limit (μM)	K_m^{app} (μM)	Sensitivity (A/(M·cm^2))	Response time (s)
Hb/ZnO-MWCNTs/Nafion*	0.2–12	0.084	82.8	1.31	3
Hb/ZrO_2/DMSO [45]	1.5–30.2	0.14	310	0.74	na
Hb/carbon nanotube [36]	210–900	9	675	na	7
Hb/polyacrylamide [3]	15–180	8	1200	na	na
{ Hb/TiO_2 }$_{15}$ [52]	1–190	na	na	2.85×10^{-3}	3.5
Hb/α-ZrP [53]	0.2–10.8	0.07	123	na	na
Hb/ionic liquid/carbon ionic liquid electrode [54]	100–5000	40	7500	na	na

*This work. na, not available.

3.6. Stability and reproducibility

The stability of the biosensor was investigated by recording a cyclic voltammogram of Hb/ZnO-MWCNTs/Nafion/GCE in 0.1 M PBS (pH 7.0). After 100 successive potential scans, the cathodic current of composite film modified electrode decreased only 3.4%. The storage stability of the composite film was also tested, and after storing it in a refrigerator (4 °C) in a dry state for 1 month, it retained 93% of the initial current response. The good long-term stability could be attributed to the efficient biocompatibility and stability of the hybrid material. The fabrication of five electrodes, made independently, showed an acceptable reproducibility with the RSD of 3.6% for the current determination of 10 μM H_2O_2.

4. Conclusions

Hb was successfully immobilized at GCE modified with a new ZnO-MWCNTs/Nafion inorganic–organic composite film. Direct electron transfer was realized between Hb and the GCE surface due to the synergic effect of ZnO-MWCNTs and Nafion. Hb in the three-dimensional structure retained its near-native conformation. This biosensor had high stability and shows highly catalytic activity to TCA and H_2O_2. The hybrid material ZnO-MWCNTs/Nafion can provide a good electrochemical sensing platform for redox proteins and have wide applications in biosensors and biocatalysis.

References

[1] Z. Zhang, S. Chouchane, R.S. Magliozzo, J.F. Rusling, Direct voltammetry and catalysis with mycobacterium tuberculosis catalase–peroxidase, peroxidases, and catalase in lipid films, Anal. Chem. 74 (2002) 163–170.
[2] Z. Lu, Q. Huang, J.F. Rusling, Films of hemoglobin and didodecyldimethylammonium bromide with enhanced electron transfer rates, J. Electroanal. Chem. 423 (1997) 59–66.
[3] X. Zeng, W. Wei, X. Li, J. Zeng, L. Wu, Direct electrochemistry and electrocatalysis of hemoglobin entrapped in semi-interpenetrating polymer network hydrogel based on polyacrylamide and chitosan, Bioelectrochemistry 71 (2007) 135–141.
[4] X. Lu, J. Hu, X. Yao, Z. Wang, J. Li, Composite system based on chitosan and room-temperature ionic liquid: direct electrochemistry and electrocatalysis of hemoglobin, Biomacromolecules 7 (2006) 975–980.
[5] Q.W. Li, G.A. Luo, J. Feng, Direct electron transfer for heme proteins assembled on nanocrystalline TiO_2 film, Electroanalysis 13 (2001) 359–363.
[6] C. Fan, H. Wang, S. Sun, D. Zhu, G. Wagner, G. Li, Electron-transfer reactivity and enzymatic activity of hemoglobin in a SP Sephadex membrane, Anal. Chem. 73 (2001) 2850–2854.
[7] Y. Yan, W. Zheng, M. Zhang, L. Wang, L. Su, L. Mao, Bioelectrochemically functional nanohybrids through co-assembling of proteins and surfactants onto carbon nanotubes: facilitated electron transfer of assembled proteins with enhanced faradic response, Langmuir 21 (2005) 6560–6566.
[8] H. Liu, N. Hu, Comparative bioelectrochemical study of core-shell nanocluster films with ordinary layer-by-layer films containing heme proteins and $CaCO_3$ nanoparticles, J. Phys. Chem. B 109 (2005) 10464–10473.
[9] D. Shan, E. Han, H. Xue, S. Cosnier, Self-assembled films of hemoglobin/laponite/chitosan: application for the direct electrochemistry and catalysis to hydrogen peroxide, Biomacromolecules 8 (2007) 3041–3046.
[10] J.J. Feng, G. Zhao, J.J. Xu, H.Y. Chen, Direct electrochemistry and electrocatalysis of heme proteins immobilized on gold nanoparticles stabilized by chitosan, Anal. Biochem. 342 (2005) 280–286.
[11] L. Zhao, H. Liu, N. Hu, Electroactive films of heme protein-coated multiwalled carbon nanotubes, J. Colloid Interface Sci. 296 (2006) 204–211.
[12] H. Zhou, X. Gan, T. Liu, Q. Yang, G. Li, Effect of nano cadmium sulfide on the electron transfer reactivity and peroxidase activity of hemoglobin, J. Biochem. Biophys. Meth. 64 (2005) 38–45.
[13] Z. Dai, S. Liu, H. Ju, H. Chen, Direct electron transfer and enzymatic activity of hemoglobin in a hexagonal mesoporous silica matrix, Biosens. Bioelectron. 19 (2004) 861–867.
[14] W. Zheng, Y.F. Zheng, Gelatin-functionalized carbon nanotubes for the bioelectrochemistry of hemoglobin, Electrochem. Comm. 9 (2007) 1619–1623.
[15] P.M. Ajayan, Nanotubes from carbon, Chem. Rev. 99 (1999) 1787–1800.
[16] Z. Deng, M. Chen, G. Gu, L. Wu, A facile method to fabricate ZnO hollow spheres and their photocatalytic property, J. Phys. Chem. B 112 (2008) 16–22.
[17] E. Topoglidis, A.E.G. Cass, B. O'Regan, J.R. Durrant, Immobilisation and bioelectrochemistry of proteins on nanoporous TiO_2 and ZnO films, J. Electroanal. Chem. 517 (2001) 20–27.
[18] Y.L. Liu, Y.H. Yang, H.F. Yang, Z.M. Liu, G.L. Shen, R.Q. Yu, Nanosized flower-like ZnO synthesized by a simple hydrothermal method and applied as matrix for horseradish peroxidase immobilization for electro-biosensing, J. Inorg. Biochem. 99 (2005) 2046–2053.

[19] F. Zhang, X. Wang, S. Ai, Z. Sun, Q. Wan, Z. Zhu, Y. Xian, L. Jin, K. Yamamoto, Immobilization of uricase on ZnO nanorods for a reagentless uric acid biosensor, Anal. Chim. Acta 519 (2004) 155–160.
[20] G. Zhao, J.J. Xu, H.Y. Chen, Interfacing myoglobin to graphite electrode with an electrodeposited nanoporous ZnO film, Anal. Biochem. 350 (2006) 145–150.
[21] G. Guo, J. Guo, D. Tao, W.C.H. Choy, L. Zhao, W. Qian, Z. Wang, A simple method to prepare multi-walled carbon nanotube/ZnO nanoparticle composites, Appl. Phys. A 89 (2007) 525–528.
[22] C.P. Andrieux, P. Audebert, B. Divisia-Blohorn, P. Aldebert, F. Michalak, Electrochemistry in hydrophobic nafion gels: part 1. Electrochemical behaviour of electrodes modified by hydrophobic nafion gels loaded with ferrocenes, J. Electroanal. Chem. 296 (1990) 117–128.
[23] J.W. Furbee, C.R. Thomas, R.S. Kelly, M.R. Malachowski, Mediated electrochemical reduction of cytochrome *c* and tyrosinase at perfluorosulfonated ionomer coated electrodes, Anal. Chem. 65 (1993) 1654–1657.
[24] I.D. Rosca, F. Watari, M. Uo, T. Akasaka, Oxidation of multiwalled carbon nanotubes by nitric acid, Carbon 43 (2005) 3124–3131.
[25] C.S. Chen, X.H. Chen, B. Yi, T.G. Liu, W.H. Li, L.S. Xu, Z. Yang, H. Zhang, Y.G. Wang, Zinc oxide nanoparticle decorated multi-walled carbon nanotubes and their optical properties, Acta Mater. 54 (2006) 5401–5407.
[26] M.J. Zheng, L.D. Zhang, G.H. Li, W.Z. Shen, Fabrication and optical properties of large-scale uniform zinc oxide nanowire arrays by one-step electrochemical deposition technique, Chem. Phys. Lett. 363 (2002) 123–128.
[27] P. George, G. Hanania, A spectrophotometric study of ionizations in methaemoglobin, Biochem. J. 55 (1953) 236–243.
[28] L. Gao, Q. Gao, Q. Wang, S. Peng, J. Shi, Immobilization of hemoglobin at the galleries of layered niobate $HCa_2Nb_3O_{10}$, Biomaterials 26 (2005) 5267–5275.
[29] C.H. Wang, C. Yang, Y.Y. Song, W. Gao, X.H. Xia, Adsorption and direct electron transfer from hemoglobin into a three-dimensionally ordered macroporous gold film, Adv. Funct. Mater. 15 (2005) 1267–1275.
[30] A.F. Nassar, W.S. Willis, J.F. Rusling, Electron transfer from electrodes to myoglobin: facilitated in surfactant films and blocked by adsorbed biomacromolecules, Anal. Chem. 67 (1995) 2386–2392.
[31] H. Luo, Z. Shi, N. Li, Z. Gu, Q. Zhuang, Investigation of the electrochemical and electrocatalytic behavior of single-wall carbon nanotube film on a glassy carbon electrode, Anal. Chem. 73 (2001) 915–920.
[32] H. Zhang, J.J. Xu, H.Y. Chen, Electrochemically deposited 2D nanowalls of calcium phosphate-PDDA on a glassy carbon electrode and their applications in biosensing, J. Phys. Chem. C 111 (2007) 16564–16570.
[33] E. Laviron, The use of linear potential sweep voltammetry and of a.c. voltammetry for the study of the surface electrochemical reaction of strongly adsorbed systems and of redox modified electrodes, J. Electroanal. Chem. 100 (1979) 263–270.
[34] E. Laviron, General expression of the linear potential sweep voltammogram in the case of diffusionless electrochemical systems, J. Electroanal. Chem. 101 (1979) 19–28.
[35] J.J. Zhang, Y.G. Liu, L.P. Jiang, J.J. Zhu, Synthesis, characterizations of silica-coated gold nanorods and its applications in electroanalysis of hemoglobin, Electrochem. Comm. 10 (2008) 355–358.
[36] Y.D. Zhao, Y.H. Bi, W.D. Zhang, Q.M. Luo, The interface behavior of hemoglobin at carbon nanotube and the detection for H_2O_2, Talanta 65 (2005) 489–494.
[37] Y. Xian, Y. Xian, L. Zhou, F. Wu, Y. Ling, L. Jin, Encapsulation hemoglobin in ordered mesoporous silicas: Influence factors for immobilization and bioelectrochemistry, Electrochem. Comm. 9 (2007) 142–148.
[38] S. Ravindran, C.S. Ozkan, Self-assembly of ZnO nanoparticles to electrostatic coordination sites of functionalized carbon nanotubes, Nanotechnology 16 (2005) 1130–1136.
[39] A.F. Nassar, Z. Zhang, N. Hu, J.F. Rusling, T.F. Kumosinski, Proton-coupled electron transfer from electrodes to myoglobin in ordered biomembrane-like films, J. Phys. Chem. B 101 (1997) 2224–2231.
[40] H. Huang, P. He, N. Hu, Y. Zeng, Electrochemical and electrocatalytic properties of myoglobin and hemoglobin incorporated in carboxymethyl cellulose films, Bioelectrochemistry 61 (2003) 29–38.
[41] E.V. Trushina, R.P. Oda, J.P. Landers, C.T. McMurray, Determination of nitrite and nitrate reduction by capillary ion electrophoresis, Electrophoresis 18 (1997) 1890–1898.
[42] A.F. Nassar, J.M. Bobbitt, J.D. Stuart, J.F. Rusling, Catalytic reduction of organohalide pollutants by myoglobin in a biomembrane-like surfactant film, J. Am. Chem. Soc. 117 (1995) 10986–10993.
[43] P. He, N. Hu, G. Zhou, Assembly of electroactive layer-by-layer films of hemoglobin and polycationic poly(diallyldimethylammonium), Biomacromolecules 3 (2002) 139–146.
[44] W. Sun, X. Li, Z. Zhai, K. Jiao, Direct electrochemistry of hemoglobin on single-walled carbon nanotubes modified carbon ionic liquid electrode and its electrocatalysis, Electroanalysis 20 (2008) 2649–2654.
[45] S. Liu, Z. Dai, H. Chen, H. Ju, Immobilization of hemoglobin on zirconium dioxide nanoparticles for preparation of a novel hydrogen peroxide biosensor, Biosens. Bioelectron. 19 (2004) 963–969.
[46] A.A. Karyakin, E.E. Karyakina, L. Gorton, Amperometric biosensor for glutamate using Prussian blue-based "artificial peroxidase" as a transducer for hydrogen peroxide, Anal. Chem. 72 (2000) 1720–1723.
[47] R.A. Kamin, G.S. Wilson, Rotating-ring-disk enzyme electrode for biocatalysis kinetic-studies and characterization of the immobilized enzyme layer, Anal. Chem. 52 (1980) 1198–1205.
[48] G. Zhao, J.J. Feng, J.J. Xu, H.Y. Chen, Direct electrochemistry and electrocatalysis of heme proteins immobilized on self-assembled ZrO_2 film, Electrochem. Comm. 7 (2005) 724–729.
[49] A. Salimi, R. Hallaj, S. Soltanian, Immobilization of hemoglobin on electrodeposited cobalt-oxide nanoparticles: direct voltammetry and electrocatalytic activity, Biophys. Chem. 130 (2007) 122–131.
[50] D. Shan, S. Wang, H. Xue, S. Cosnier, Direct electrochemistry and electrocatalysis of hemoglobin entrapped in composite matrix based on chitosan and $CaCO_3$ nanoparticles, Electrochem. Comm. 9 (2007) 529–534.
[51] H.N. Choi, M.A. Kim, W.Y. Lee, Amperometric glucose biosensor based on sol–gel-derived metal oxide/Nafion composite films, Anal. Chim. Acta 537 (2005) 179–187.
[52] H.Y. Lu, J. Yang, J.F. Rusling, N.F. Hu, Vapor-surface sol-gel deposition of titania alternated with protein adsorption for assembly of electroactive, enzyme-active films, Electroanalysis 18 (2006) 379–390.
[53] Y. Liu, C. Lu, W. Hou, J. Zhu, Direct electron transfer of hemoglobin in layered α-zirconium phosphate with a high thermal stability, Anal. Biochem. 375 (2008) 27–34.
[54] A. Safavi, N. Maleki, O. Moradlou, M. Sorouri, Direct electrochemistry of hemoglobin and its electrocatalytic effect based on its direct immobilization on carbon ionic liquid electrode, Electrochem. Comm. 10 (2008) 420–423.